Original article

Journal of High School Science

Starlink satellite collision probability simulation based on a simplified geometry model

Li C.H

Submitted: August 10, 2023, Revised: version 1, October 23, 2023
Accepted: October 27, 2023

Abstract

In this paper, a model based on simplified geometry is introduced to give a conservative collision probability prediction for a Starlink satellite in its most densely clustered region. Using the model, the probability of collision was found to be 8.5 X 10^{-4}. The predicted collision probability increased nonlinearly with the increased set safety distance. This simple model provides evidence that the continuous development of maneuver avoidance systems is necessary for the future of the orbital safety of satellites under the harsher Lower Earth Orbit environment.

Keywords

Starlink, Satellite, Collision, Low Earth Orbit, SpaceX, Space debris, Monte Carlo method, NASA, Collision avoidance system, Propulsive maneuver

---

Cheuk Hon Li, Harrow International School, 38 Tsing Ying Rd, Tuen Mun, Hong Kong. 0220202898@harrowschool.hk

1.0 Introduction

With the advancement of modern rocket technology, ever more satellites are being sent to low Earth orbit (LEO) to operate various missions. Satellites play an essential role in different fields of society. Since the first artificial satellite was launched in 1957, there have been a steady stream of satellite launches. As examples, the detection of crop growth situations and inspection of particular commercial crops is performed by satellites. Satellites can monitor urban traffic flow in peak periods and navigate for all car users. As of April 30, 2022,, there were about 5,465 satellites functioning in space; out of them, 4,700 satellites orbiting in LEO (1). As one of the largest commercial satellite companies, SpaceX owns over 3,300 Starlink satellites in LEO (2). While the Federal Communications Commission (FCC) only permits launching up to 12,000 satellites, Space X has plans to launch about 42,000 satellites in LEO (3). However, with the increased number of satellites, space debris has also increased significantly. This raises the probability of collisions in LEO and threatens satellite life-span.

According to the ESA's MASTER-8 model, there are 36,500 objects larger than 10 cm in the current Earth orbit and over 1.3 million between 1 mm and 1 cm (4). This huge number of debris particles significantly endangers the safety of the existing operating satellites in every Earth orbit. There are several leading causes of space debris formation. About 39% of current space debris is generated due to the explosion of undisposed fuel on inactivated satellite or rocket components. Intentional breakup of satellites accounts for 24% of total space debris, and several collisions observed contribute about 9% (5) of current space debris. Figure 1 indicates that the number of tracked space debris objects has increased rapidly since 1960, posing a significant risk to satellites. As evident from Figure 1, the overall trend of debris numbers is increasing, which can be observed with the recent year's data (6).

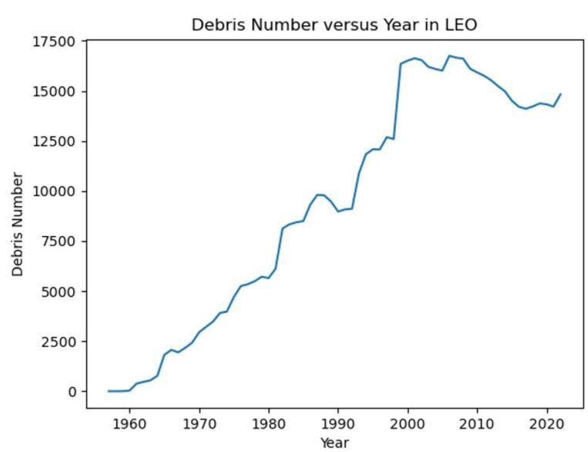

Figure 1. Number of debris objects observed since 1960

1.1 *Problem statement*

The rapid increase in space junk increases the probability of collisions of commercial satellites with various space debris. For instance, on February10, 2009, the commercial satellite Iridium-33 and the Cosmos-2251, a decommissioned Russian military spacecraft, collided. Over 2,201 debris fragments (7) were tracked from then until June 2012, and clouds of the fragments were detected after the collision, as shown in Fig (2). It is predicted that the debris from Cosmos-2251 will stay in orbit for the next 20–30 years and debris from Iridium-33 will remain for over 100 years in LEO.

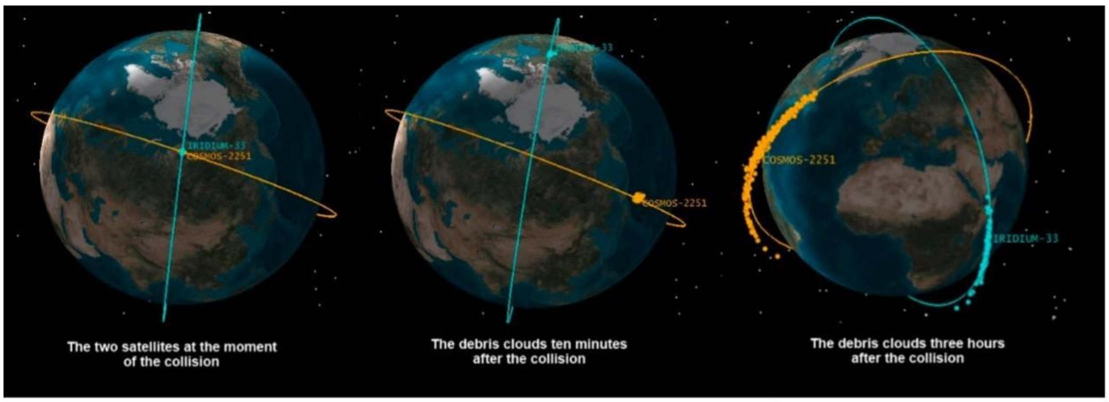

Evolution of the debris clouds over the first three hours [6]

Figure 2. The trajectory of debris created by collision of Iridium-33 and Cosmost-2551 (direct reference of pictures approved by the original author)

Although the collision probability is almost zero after regulation of a satellite, the collision probability still exists when the satellite encounters random space junk. Faced with this situation, the satellite needs to perform avoidance maneuvers to reduce the risk of collision (8). However, any maneuvers consume fuel and reduce the satellite's lifetime in orbit. Therefore, it is important to effectively predict the collision probability and adjust in advance for the on-orbit life of satellites and the space safety of LEO. Collision probability prediction is especially necessary for Starlink satellites, one of the largest satellite collections. Haicheng et al. Predicted the Starlink satellite in-orbit secondary collision risk with space debris using a matrix, integration, and MASTER-8 model (9). They focussed on predicting the collision probability of Starlink satellites at the most densely clustered altitude in LEO. However, there is still a lack of research focused on Starlink collision for LEO collision.

1.2 *Model formulation*

A conventional method used to predict the necessity of maneuver avoidance determines when a tracked object is expected to cross a keep-out zone of 5 X 2 X 2 km centered on the Orbiter. However, this method does not predict collision probability between debris and satellites. Significant progress has been made in the collision probability calculation problem using complex algorithms and considerable computing power. First, researchers examine the three-dimensional probability density. To reduce computation, the model assumes the satellite to be spherical so as to obtain a two-dimensional integral over a circular region. In 2001, Patera et al. found that instead of integrating over an area, integrating around its edge could speed up processing by decreasing the number of times the integrand needed to be evaluated (10). This method does not need to assume a spherical shape, hence leading to more accurate results. Inspired by this research, this paper reduced three-dimensional space into two-dimensional space by projecting a cross-sectional area around the circular path.

Instead of using a complex series of calculus and matrices to predict the probability of collision, this paper adopted a spatial geometrically based approach to predict a very conservative collision probability. Since the method is relatively coarse compared to existing models, it cannot predict collision probability with 100% accuracy. However, this model can provide a rough estimate of the collision probability quickly because it does not require complex computation and data. Furthermore, with the advantage of using the geometric properties of the space for calculation, this model can be better understood by non-experts unfamiliar with the field.

1.3 *Section review*

This paper aimed to investigate the collision probability in regions with a high density of Starlink satellites. Specifically, the focus was on the LEO region where Starlink is distributed most densely. Two scenarios were investigated: the first being the collision probability of Starlink satellites with debris in 2022 at an altitude of 539-561 km; the second being the average collision probability of Starlink satellites between 2022 and 2040 at an altitude of 525-535 km, assuming there are 10,080 satellites in the region described. In Section 2, a systematic analysis of the investigated environment is introduced. The factors that were significant for the research, such as the distribution of the satellites and prediction of the number of debris objects, are discussed in the section. Section 3 focuses on the modeling: a probability model based on the Monte Carlo method approximated the collision probability between Starlink satellites and debris at the selected altitudes. The section describes how to gradually simplify a physical problem and convert it into a mathematical probability problem while considering a certain accuracy threshold. Section 4 analyzes the experimental results of the model. The uncertainty caused by model simplification is also discussed, and an analysis of the uncertainty is presented. Finally, Section 5 reviews the analysis and experiments conducted throughout the paper and evaluates the overall advantages and disadvantages of the model. The effectiveness of improving the model to increase the prediction of the collision probability is also discussed.

2.0 System analysis

2.1 *Space environment introduction*

In this paper, a standard from the National Aeronautics and Space Administration (NASA) was used to divide Earth satellites, which are defined at an altitude of 160-2,000 km. The Earth radius chosen in this paper was the equatorial radius of Earth, which is 6,378.13 km. This paper focussed on the distribution of SpaceX satellites and debris in LEO. Debris and satellite density were calculated for the data set established in this section.

2.2 *Debris distribution*

This paper only focussed on important information that affected the prediction of collision of probability, such as the launch year of the satellites, decay year of debris, and apogee and perigee of debris. The debris data was obtained from the United States Space Command (USSPACECOM) (6), which included all the information about the debris that has appeared in LEO since 1957. The total debris number was the sum of debris objects and rocket bodies. In 2022, 14,825 pieces of debris were observed in LEO, with 3,032 pieces of debris being in the region of 539-561 km. Since the debris trajectory is uncertain and random, it was assumed in this paper that the debris in LEO is uniformly distributed. Therefore, the density of LEO debris could be derived from the density formula. Debris density at the altitude of 539-561 km could be obtained using equation 1. In this equation, N_{debris} is the number of satellites in the selected region, R_{Earth} is the radius of Earth, $H_{high}$is the higher altitude of the selected region, and H_{low} is the lower altitude of the selected region.

$$\rho_{debris}=\frac{N_{debris}}{\frac{4}{3}\pi\left[\left(R_{Earth}+H_{high}\right)^3-\left(R_{Earth}-H_{low}\right)^3\right]} \qquad \text{equation 1}$$

To model the debris density in the future, the number of debris objects in consecutive years in the short future needed to be predicted. This prediction was based on the number of debris objects tracked in the past since the first rocket was launched. Figure 3 presents the debris data set that tracked objects at an altitude of 525-535 km since 1957; prediction for debris numbers in the future was based on this data.

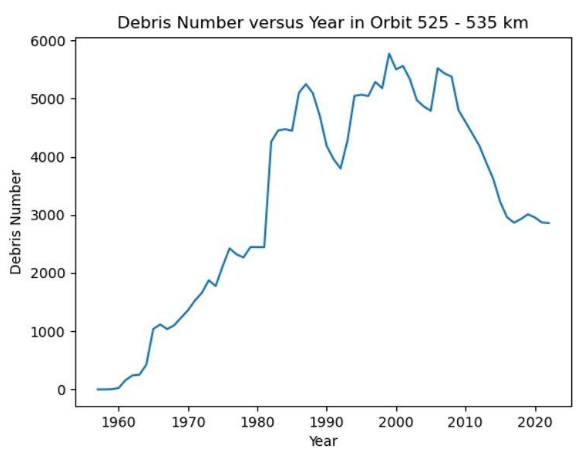

Figure 3. Number of debris objects in altitude of 525-535km since 1957

According to Figure 3, the trend of the number of debris objects can be observed from 1957 to 2022. An interpolation method could be used to process this data and then fit a curve consistent with the trend of growth to predict the number of debris objects in the future. However, an interpolation method might not always be precise enough to predict the number, especially after an extended period, as prediction numbers are based on logarithms. Instead, this paper predicted the number of debris objects in LEO over the next 18 years using a polynomial fit of the available data. The fitting curve with a polynomial degree of 3 is presented in Figure 4. The general polynomial fitting equation has a fitting model which can be written as

$$f(x) = w_0 + w_1 x + w_2 x^2 + w_3 x^3 + w_4 x^4 + ¿ \ldots . w_n x^n$$

For the third-degree polynomial, the fitting equation of the predicting curve was:

$$f(x) = 4.33 \times 10^{-5} - 6.37 \times 10^{-3} x + 2.84 \times 10^{-1} x^2 + 4.59 x^3$$

To obtain the fitted curve, the number of debris objects in the first three years since 1957 was not considered as the data affected the gradient of the fitted curve, exaggerating the number for the predicted debris number. From the adjusted fitting curve, the number of debris objects in LEO in the next 18 years was predicted as shown in Figure 5, where the predicted debris number at the region increased from 3,158 in 2022 to 6,287 in 2040.

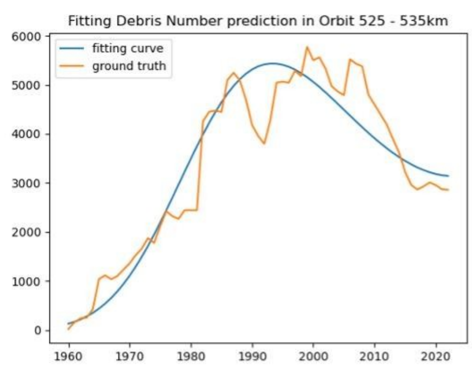

Figure 4. The fitting curve of debris number against years since 1960

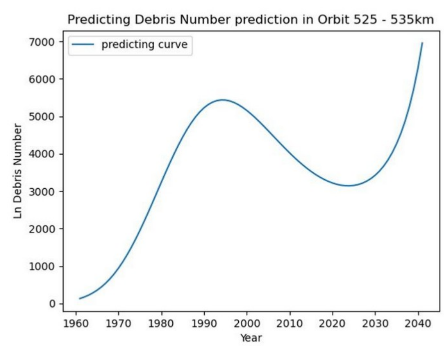

Figure 5: Predicted number of debris objects from 1960 to 2040

2.3 *Distribution of SpaceX satellites*

Starlink has 12,000 satellites ready to launch and has applied to launch 30,000 more in the future. This sets an upper bound for the number of Starlink satellites in LEO. There are currently over 3,300 Starlink satellites in LEO, including those just launched. Most Starlink satellites orbit between latitudes 53 to -53 degrees, with only about 3% of satellites crossing outside of those latitudes (11). It is assumed that the Starlink satellites do not have an autonomous collision avoidance system under the model presented in this paper.

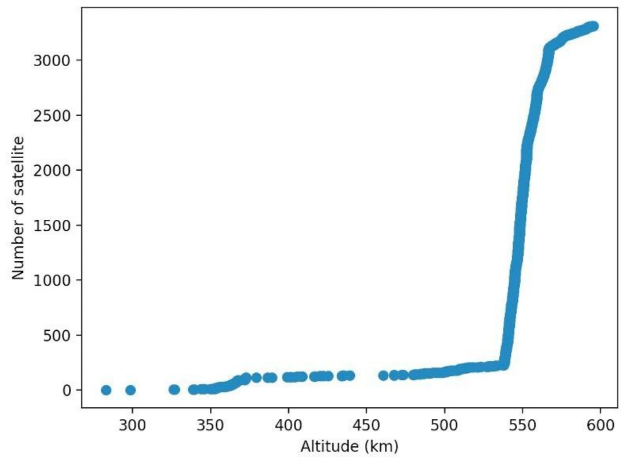

Figure 6. Distribution of Starlink satellites by altitude

Figure 6 shows that 89.7% of current Starlink satellites were at an altitude of 530-600 km, where this research mainly focuses. As seen in Figure 7 below, around 3,100 Starlink satellites lie between a 500-600 km altitude, and 2,442 Starlink satellites were distributed at an altitude of 539-561 km. An initial model was constructed on the attitude between 539-561 km, as Starlink satellites operate most densely in this altitude region.

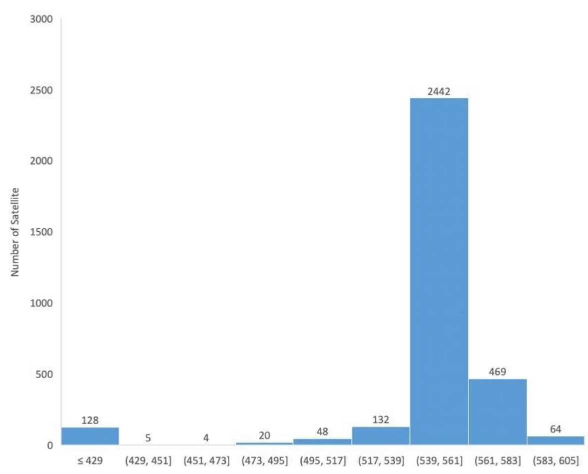

Figure 7. Distribution of Starlink satellite altitude

Since the distribution and orbits of the satellites are relatively fixed, the density equation 2 was used to estimate the distribution density of Starlink satellites at a given altitude and derive the number of satellites present in the set height. In the formula, $N_{satellite}$ is the number of satellites in the selected region, $R_{Earth}$is the radius of Earth, H_{high} is the higher altitude of the selected region, and N_{low} is the lower altitude of the selected region.

$$\rho_{satellite} = \frac{N_{satellite}}{\frac{4}{3}\pi\left[\left(R_{Earth} + H_{high}\right)^3 - \left(R_{Earth} - H_{low}\right)^3\right]} \qquad \text{equation 2}$$

2.4 *Dimensions and orbital period of satellites*

All the current Starlink satellites in the LEO are generation 1 (Gen 1). A Gen 1 Starlink satellite has a length of approximately 2.8 meters, width of 1.4 meters, and height of approximately 0.2 m [12]. The surface area of the Space X satellite solar panel is 23.657 (from the DISCOB web); the solar length of the panel is 8.45 m and the longest side of the satellite is 8.65 m. Approximation for the collision distance was considered by using the dimensions of the satellite. According to the data from 3,269 Starlink satellites, the average orbit period for a functional satellite is 95.06 minutes. This information was used to calculate the length of time for a collision to occur after the construction of the model.

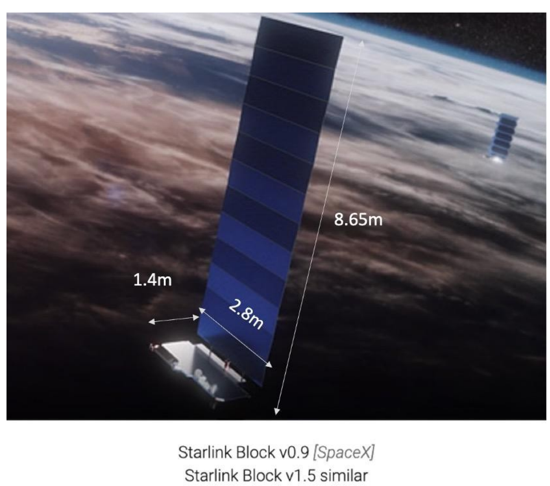

Figure 8. Gen 1 Starlink satellite (Picture reformatted from [12])

3.0 Probability model based on the Monte Carlo method

3.1 *System model*

This paper proposed a model that utilized the Monte Carlo method for practical application in LEO , which included the Starlink satellites. The study focussed on a specific altitude within LEO by dividing LEO into smaller sections of independent space for investigation purposes. The model was designed to maintain a constant satellite height during steady-state operation, disregarding physical parameters such as angular momentum and trajectory. To simulate the satellite coordinates in space, the satellite was approximated as a sphere with a fixed radius, and the sphere's center point was used as the polar coordinates to determine the position of satellites relative to the independent space. Similarly, space junk was approximated as a sphere with a uniform radius, and the center polar coordinates of the sphere were utilized to determine the position of the satellite with respect to the independent space. The number of debris objects and satellites in the set region was determined by debris and satellite density corresponding to the investigating region.

3.2 *Application of the Monte Carlo method*

Having obtained the density of the satellite and debris, an initial model was constructed. The first step was to select the altitude interval to be investigated. Using the center of Earth as the center; a hollow sphere is formed, as shown in Figure 9. The thickness of the 'sphere shell' was the selected altitude interval where the difference in the altitude of the 'sphere shell' was defined by 'd'. The distance from the center of the Earth to the lower bound of the 'sphere shell' was defined by 'R,' and the total volume of the 'sphere shell' was the volume of the selected altitude interval as shown in Figure 10.

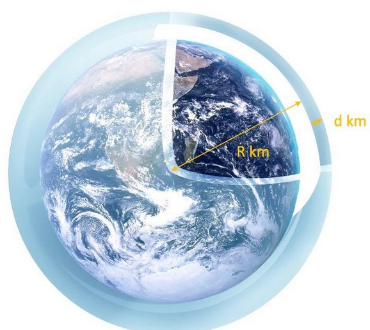

Figure 9. Starlink orbit shell around the Earth

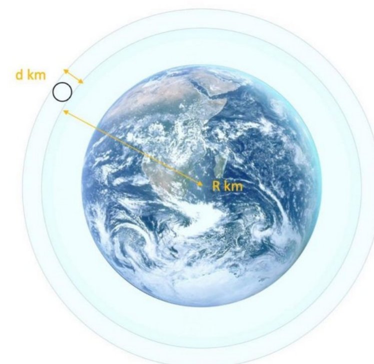

Figure 10. Cross-sectional view of orbit

To simplify the model, a circle was constructed inside the shell where the circle's diameter was 'd'. The circle was extended around the center of the shell to create a doughnut-shaped space. When stretched out, this doughnut-shaped space formed a cylinder space, as shown in Figure 11. The height of the cylinder form was the circumference of the 'doughnut' shape. That is also the circumference of the sphere form with a radius from the center of the Earth to the upper bound of the 'sphere shell.' To determine the volume of the cylinder space form, equation 3 was used. R is the distance from the center of Earth to the lower boundary of the 'sphere shell,' and d is the diameter of the cylinder form. The estimated number of Starlink satellites and debris objects in selected space was thus obtained from equations 4 and 5.

$$V_{space} = 2\pi(R+d) * \pi \qquad \text{equation 3}$$

$$S_{debris} = \rho_{debris} \times V_{space} \qquad \text{equation 4}$$

$$S_{satellite} = \rho_{satellite} \times V_{space} \qquad \text{equation 5}$$

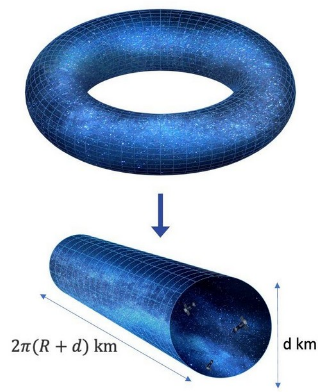

Figure 11. Uniform cylinder space for cross-sectional direction

The model assumed that the satellite's orbital altitude did not change during the operation cycle, hence a single satellite moved in a straight line in the cylindrical space of the model. The model assumed it was a stationary sphere in the cylinder for any debris. A circle was drawn with a radius defined as a ‘safety distance’ with the center point of the satellite as the center of the circle. A smaller cylinder, defined as a ‘safety zone,’ was obtained after the satellite moved from one side of the cylinder to the other side. The model defined whether the satellite collided with the debris by determining whether the sphere represented by the debris was in the safety zone formed by the movement of a satellite in cylindrical space. If the sphere represented by the debris was in the safety zone, the model determined that the satellite and the debris would collide.

After the previous settings, further simplification was performed, converting the model from 3D to a more concise 2D model. Since the orbit of the satellite in the cylindrical space was known to be a straight line, the determination of whether the debris collides was made by observing whether the sphere represented by the debris appeared in the safety zone formed by the satellite. The cylinder could then be compressed, and as the thickness of the cylindrical space approached zero, a circle of diameter d km, as shown in Figure 12, was formed.

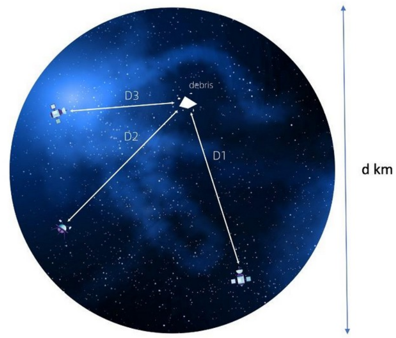

Figure 12. Simplification of 3D space to 2D

The model's determination of whether a collision would occur was more straightforward under 2D. As shown in Figure 12, it was assumed that three satellites were on a circle with a diameter of d km, and their distance from the debris randomly appearing on the circle was D1, D2, and D3. The model determined that a collision would occur when the distance between D1, D2, or D3 was less than the specified safe distance. Polar coordinates determined the satellite's position and random debris on the circle. At the start of each orbit, a random polar coordinate was assigned to the satellites and debris, and random functions changed the coordinate after each satellite completed one full orbit of motion. Since the selected cylindrical space was random in the 'spherical shells,' the positions of the satellite and debris changed after each orbit period. Although the positions of the satellite and debris changed randomly, they were still within the space of the circle formed by the model, as Figure 12 shows, and not beyond it, as this could cause changes in the distribution density of the debris and satellite.

4.0 Simulation set up and scenario

4.1 *Simulation setup*

Considering that the radius of the sphere formed by the satellite and the sphere formed by the random debris was close to 20 meters, the relative velocity between debris and a Starlink satellite in LEO was approximately 10 to 15 km per second. There existed an uncertainty in the position of the satellites using the simplified simulation model. Therefore, the model set up a 'safety distance' to define whether or not a collision would occur. In this model, 100 m was used as the standard safety distance. Further analysis was performed on the effect of varying the safety distance on the collision probability.

4.2 *First scenario: constant debris numbers*

The first scenario set a constant debris number for the model and the satellite. During the repeat of the experiment, the number of debris objects in the model did not change with time. The number of debris objects in LEO to estimate the corresponding debris density used the 2022 data, which was 3,042. The number of satellites used to estimate satellite density was 2,442. It was assumed that the distribution of satellites and debris was random in the given regions. This model selected the altitude where Starlink satellite distribution was the most dense. According to the altitude distribution of Starlink satellites in LEO, the range 539-561 km is used. The probability of collision was defined as the average collision probability every period around Earth for a Starlink satellite, which was also the average collision probability over 90 minutes. By counting the average collision events that occured during the 100,000 periods of the orbit, the probability of collision of Starlink satellites with debris over 90 minutes was determined from equation 6, where $P_{collision}$ is collision probability, and $N_{collision}$ is the average collision count over 100,000 periods.

$$\frac{P_{collision}}{90\,mins} = \frac{N_{collision}}{100{,}000} \qquad \text{equation 6}$$

4.3 *Second scenario: increment of satellites and debris number*

The second scenario considered the increment of satellites and debris with time. This model focussed on the altitude range where the Starlink satellites were predicted to be the most densely distributed in the future. The number of debris objects in LEO to estimate the corresponding debris density used the data from the predicted number of debris objects from 2022 to 2040, which increased from 3,158 to 6,287. The number of satellites used to estimate satellite density was 10,080. It was assumed that the distribution of satellites and debris was even in the given region. This model selected the altitude where Starlink satellites gather most densely for the experiment, which was 525-535 km..

5.0 Results

From the data set collected, debris density in the altitude of 539-561 km was calculated to be 2.285×10^{-7} debris/km^3 from equation 1.

5.1 *First scenario*

The density of Starlink satellites at this altitude is 1.840×10^{-7} Satellite/km^3. Depending on the model setup, a cylinder with a radius of 11 kilometers and a length of 43,486 kilometers was formed. Based on the model, at an altitude of 539-561 km, each 'cylinder' contained 2.813 Starlink satellites and 3.493 debris objects. In the simplified model, two circles with a radius of 10 meters per circle were placed randomly in a radius of 11 kilometers to represent the respective positions of the two satellites with an additional 0.813 probability of having an extra circle with a radius of 10 meters to represent the extra one satellite that could appear. Meanwhile, there were three additional circles each with a radius of 0.1 m to represent the positions of three pieces of debris, and a 0.493 probability that an extra circle with a radius of 0.1 m would appear to represent the extra piece of debris. Positions of the circles were randomly assigned to represent the position of random debris and satellites.

With relevance to the model in the first scenario where the safety distance was 100 m, the average count for the number of collisions was determined to be 84.84 per 100,000 periods. Under the definition of collision probability set in the scenario, the collision probability was determined to be 8.484 X 10^{-4}. Figure 13 shows how the collision count predicted change as safety distance varied from 50 to 500 meters. Figure 13 shows a non-linear growth when the safety distance increased from 50 m to 500 m with the same experimental setup in scenario one. With the safety distance of 50 m, average collision counts were 21.75,. These increased to 2140.37 when the safety distance was 500 m. The corresponding collision probability increased from 2.174 X 10^{-4} to 2.140 X 10^{-2}.

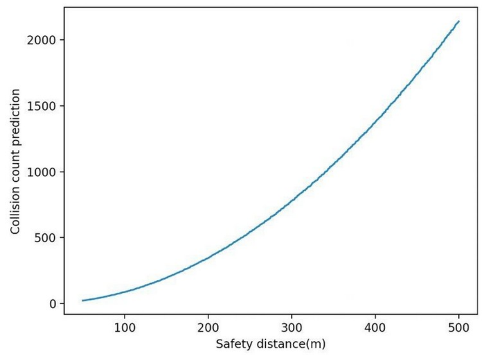

Figure 13. Collision count prediction against safety distance for the first scenario.

5.2 *Second scenario*

The density of Starlink satellites at this altitude was 1.681 X 10^{-7} satellite/km^3 . Depending on the model setup, a cylinder with a radius of 5 kilometers and a length of 43,360 kilometers was formed. Considering the increased numbers of debris objects with the time change, the 100,000 orbit period of Starlink satellites was calculated to be approximately 18 years. Taking the average for the predicted number of debris objects since 2022, the average estimated debris number was 3,949.178. This led to the debris density in the selected region. The cylinder form contained 5.299 Starlink satellites and 2.076 debris objects. In the simplified model, five circles with a radius of 10 meters per circle were placed randomly in a radius of 5 kilometers to represent the respective positions of the five satellites with an additional probability of 0.299 for an extra satellite to appear. Meanwhile, there were two additional circles, each with a radius of 0.1 m to represent the positions of two pieces of debris, and a 0.076 probability that an extra circle with a radius of 0.1 m would appear to represent the extra piece of debris. Positions of the circles were randomly assigned to represent the position of random debris and satellites.

For the model in the second scenario, where the safety distance was 100 m, the average count for the number of collisions was 452.99 per 100,000 periods. Under the definition of collision probability set in the scenario, the collision probability was 4.530 X 10^{-3}. Figure 14 shows how the predicted collision counts changed as the safety distance varied in the range from 50 to 500 meters. Figure 14 shows a non-linear growth when the safety distance increased from 50 m to 500 m with the same experimental setup as in scenario one. With the safety distance of 50 m, the average collision count was 117.33, which increased to

11,157.32 when the safety distance was 500 m. The corresponding collision probability increased from 1.173 X 10^{-3} to 1.116 X 10^{-1}.

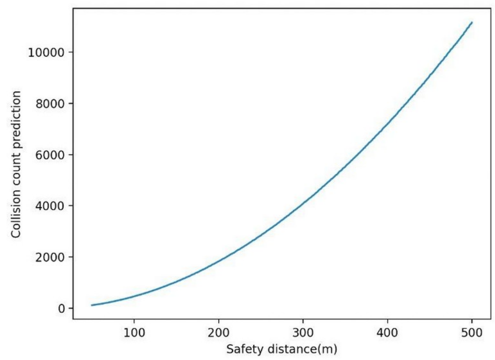

Figure 14. Average collision count against safety distance for the second scenario

When comparing the data from both scenarios, in the same safe distance, the growth rate of predicted collision counts in scenario 2 was found to be significantly greater than that in scenario 1, as shown in Figure 15. Within the set safe distance of 50 to 500 meters, the average number of collisions in scenario 2 was almost five times that in scenario 1 at the same safety distance. Considering the uncertainty brought by the estimation and approximation of the model, an uncertainty test was also applied to the prediction of the collision counts. Using standard error, a graph of standard error against safety distance set from 50 to 500 m was plotted, as shown in Figure 15. For the first scenario, at the safety distance of 50 m, the standard error was 0.4723, where the error increased to 4.3024 when the safety distance was set at 500 m. For the second scenario, the standard error at 50 m was 0.9650 and increased to 11.0737 when the safety distance was set at 500 m. Although the standard error increased linearly along the increasing safety distance for both scenarios, this did not affect the non-linear growth for the collision counts when the safety distance increased.

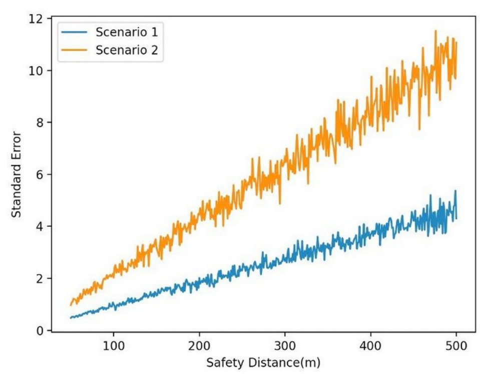

Figure 15. Standard error with safety distance increases for both scenarios

6.0 Conclusion

This paper estimated the current probability of debris colliding with Starlink satellites at the altitude where the satellites are most densely clustered. The average collision probability in the next 18 years was also estimated. The model in this paper assumed that the Starlink satellite does not have an autonomous collision avoidance system and ignored the physical quantities, such as velocity and time, affecting the satellite when calculating the collision probability. The Monte Carlo method was used to estimate the probability of collision after simplification of the initial model. Considering the error caused by model simplification and approximation, the standard safety distance of the model was set to 100 meters. At altitudes of 539 -561 km, the Starlink satellite had a collision probability of 8.484 X 10^{-4} in 2022. The estimated number of collisions increased nonlinearly with the increase in safety distance. Over the next 18 years, the model predicted an average collision probability of 4.530 X 10^{-3} at an altitude of 525-535 km if the orbit was populated with the estimated number of satellites. The estimated number of collisions also presented a nonlinear increase with the increasing safety distance. In the analysis of the predicted collision counts, the standard error of the predicted collision counts increased with the increase of the safety distance. However, the error range did not affect the nonlinear increase of the predicted collision counts. It was concluded that the probability of collision increases significantly with the increased safety distance set, and the standard error of the experiment increases linearly along the increasing average collision count. In the long run, the increase of collision probability with time poses a significant risk to the safety of Starlink satellites. Therefore, it is necessary to continuously develop and improve the debris detection and collision avoidance system in the future.

The advantage of the model presented in this paper is that it used a relatively simple method and model to determine a conservative collision probability. First, a 3D collision problem was converted into 2D, which made the model easier to visualize. Second, the computation was also simplified because calculus and matrices were not required to calculate the collision probability. This method can be used to rapidly estimate the collision probability of satellites and debris within a specific chosen region. Finally, this method is suitable for the non-expert. Due to the model's simplicity, it can provide a more intuitive understanding for the general public of the probability of collision between a satellite and debris. The experiments described in the paper can also be performed on a commercial computer, making it available to the public.

Although the model can easily and quickly predict the collision probability, adjustment to improve prediction accuracy is necessary. Several methods can increase the accuracy of the model. First, the model in the paper used the average density of Starlink satellites to estimate Starlink satellites in each cylindrical space. However, because most Starlink satellites are not distributed in high and low latitudes, the density of the satellites will be different from that calculated in the paper when the 'doughnut' model space is used to simplify, resulting in a different number of satellites in each 'doughnut' space. Then, if the high and low latitude spaces are removed, the original model is also no longer a spherical shell around the Earth, resulting in a different volume of each doughnut space formed in the model. Therefore, considering the number density distribution function is necessary to improve the experimental accuracy. At the same time, more integration is required, as well as more accurate mathematical models to approximate the shell's geometrical shape.

Second, the model's definition of the collision range of the satellite and debris could be more rigorous. The collision range of this model was determined to be a collision when any debris appears in the safety zone formed in the satellite's orbit. The prerequisite is to ignore that the coordinates of the satellite change over time in cylindrical space. If the influence of time change on the real-time coordinates of the satellite is considered, it would be more accurate to use the matrix to represent the coordinates of the satellite in the cylinder space at any time and the distance between random debris and the satellite at a particular time can be calculated more accurately.

Finally, in future research, to predict the collision probability more reasonably and accurately, it is necessary to consider the collision avoidance maneuvers performed by the satellites that mitigate the probability of collision. . The Starlink satellite serves as an example. In the report from SpaceX, from June 1, 2022 – November 30, 2022, Starlink satellites performed 13,612 propulsive maneuvers, approximately 12 maneuvers per satellite (14). A collision probability calculation can occur if each maneuver means a collision or a high risk of collision. Random Starlink satellites can orbit Earth 2,880 times according to the simulation setup, hence, during six months, a random Starlink satellite has a collision probability of 4.167×10^{-3}. This result is greater than what the simulation predicted. However, it is to be noted that for Starlink satellites, if collision probability reaches above 1×10^{-5}, then maneuvers must be performed. Therefore, the actual collision risk for a Starlink satellite could be lesser than calculated above and more aligned with the simulation result. Such maneuvering would significantly reduce the likelihood of collision and should be considered in future studies.

7.0 Supplemental information

Online code database:
https://github.com/CheukHonLi/Starlink_Satellite_Probability_Collision_Model

8.0 References

1. https://www.ucsusa.org/resources/satellite-database

2. https://aviation-edge.com/spacex-satellite-tracker-api/

3. https://www.space.com/spacex-starlink-satellites.html

4. https://www.esa.int/Space_Safety/Space_Debris/Space_debris_by_the_numbers

5.https://www.esa.int/ESA_Multimedia/Images/2021/03/The_history_of_space_debris_creation#.ZFUTdpQ0wVQ.link

6. https://www.space-track.org/#catalo

7. Kelso, T. S. "Analysis of the Iridium 33-Cosmos 2251 collision." Advances in the Astronautical Sciences 135(2), (2009): 1099-1112.

8. Stevenson. M, McKnight. D, Lewis. H, Kunstadter C, Bhatia R. "Identifying the statistically-most-concerning conjunctions in leo." 2021 Advanced Maui Optical and Space Surveillance Technologies Conference (AMOS), Maui, Hawaii. 2021.

9. Haicheng. T, Xueke. C, Qinyu. Z, XinHong. L. "Satellite In-Orbit Secondary Collision Risk Assessment", International Journal of Aerospace Engineering, 2022 (2022): Article ID 6358188. https://doi.org/10.1155/2022/6358188

10. Patera, Russell P. "General method for calculating satellite collision probability." Journal of Guidance, Control, and Dynamics 24(4), (2001): 716-722.

11. https://satellitemap.space/?constellation=starlink0#

12. https://space.skyrocket.de/doc_sdat/starlink-v1-5.htm

13. https://www.nasa.gov/news/debris_faq.html

14. https://planet4589.org/astro/starsim/docs/Star2212.pdf